Supporting Information

Crystal Structure, Morphology and Surface Termination of Cyan-Emissive, 6-Monolayers-Thick $CsPbBr_3$ Nanoplatelets from X-Ray Total Scattering

Federica Bertolotti,[a,#*] Georgian Nedelcu,[b,c#] Anna Vivani,[a] Antonio Cervellino,[d] Norberto Masciocchi,[a] Antonietta Guagliardi[e*] and Maksym V. Kovalenko[b,c,*]

[a] Dipartimento di Scienza e Alta Tecnologia & To.Sca.Lab, Università dell'Insubria, via Valleggio 11, 22100 Como, Italy

[b] Department of Chemistry and Applied Biosciences, ETH Zürich, Vladimir-Prelog-Weg 1, Zürich 8093, Switzerland

[c] Laboratory for Thin Films and Photovoltaics, Empa−Swiss Federal Laboratories for Materials Science and Technology, Dübendorf 8600, Switzerland

[d] SLS, Laboratory for Synchrotron Radiation - Condensed Matter, Paul Scherrer Institut, 5232 Villigen, Switzerland

[e] Istituto di Cristallografia & To.Sca.Lab, Consiglio Nazionale delle Ricerche, via Valleggio 11, 22100 Como, Italy

* F. Bertolotti. E-mail: federica.bertolotti@uninsubria.it
* A. Guagliardi. E-mail: antonella.guagliardi@ic.cnr.it
*M.V. Kovalenko. E-mail: mvkovalenko@ethz.ch

Supplementary Figures

Figures S1-S10

Supplementary Tables

Tables S1

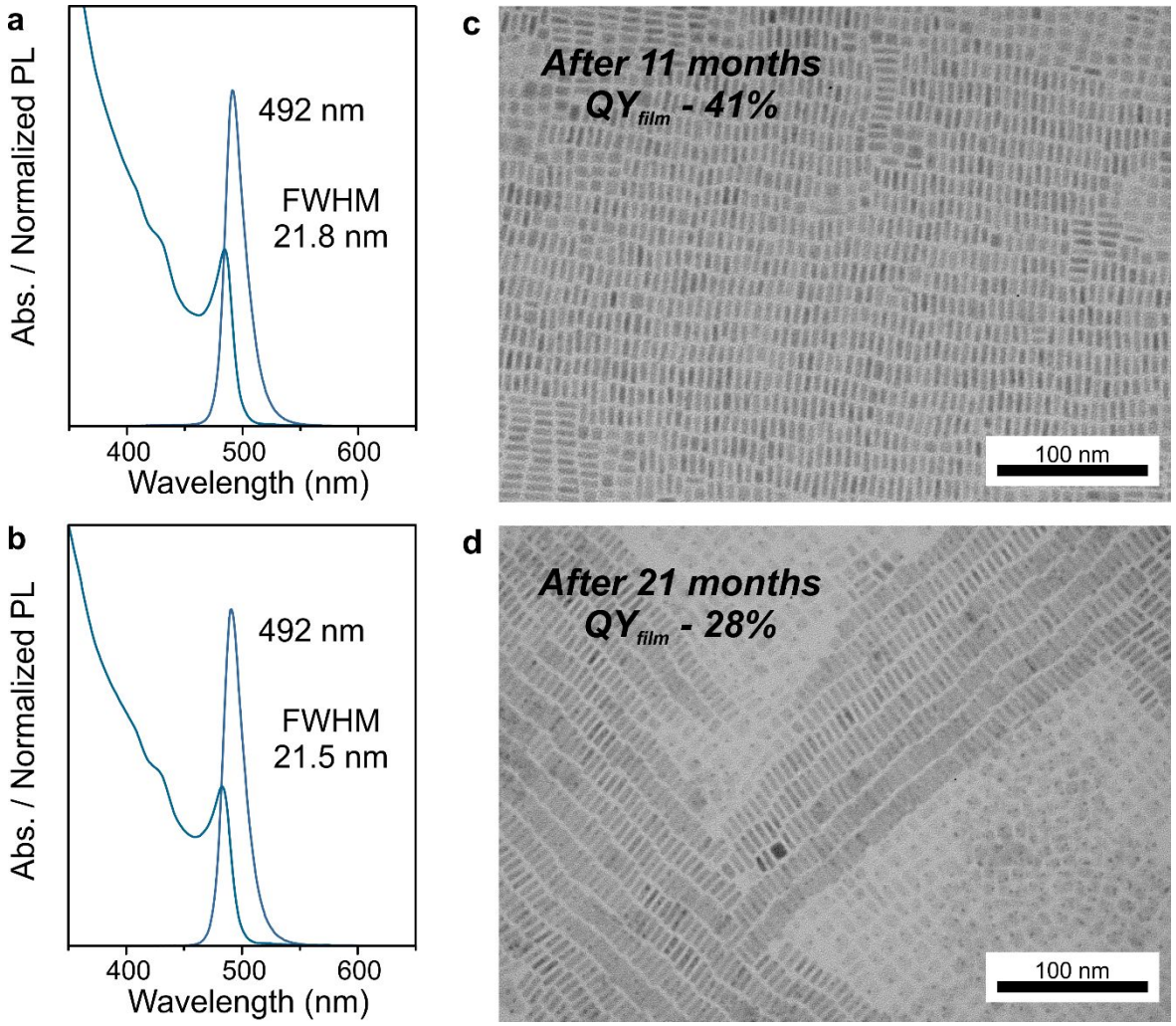

Figure S1. Absorbance and PL spectra of $CsPbBr_3$ NPLs aged for: **(a)** 11 months and **(b)** 21 months, respectively, showing the preservation of the absorbance and PL peak positions; Low-resolution TEM micrographs of the aged $CsPbBr_3$ NPLs proving the conservation of the morphology after **(c)** 11 months and **(d)** 21 months, respectively.

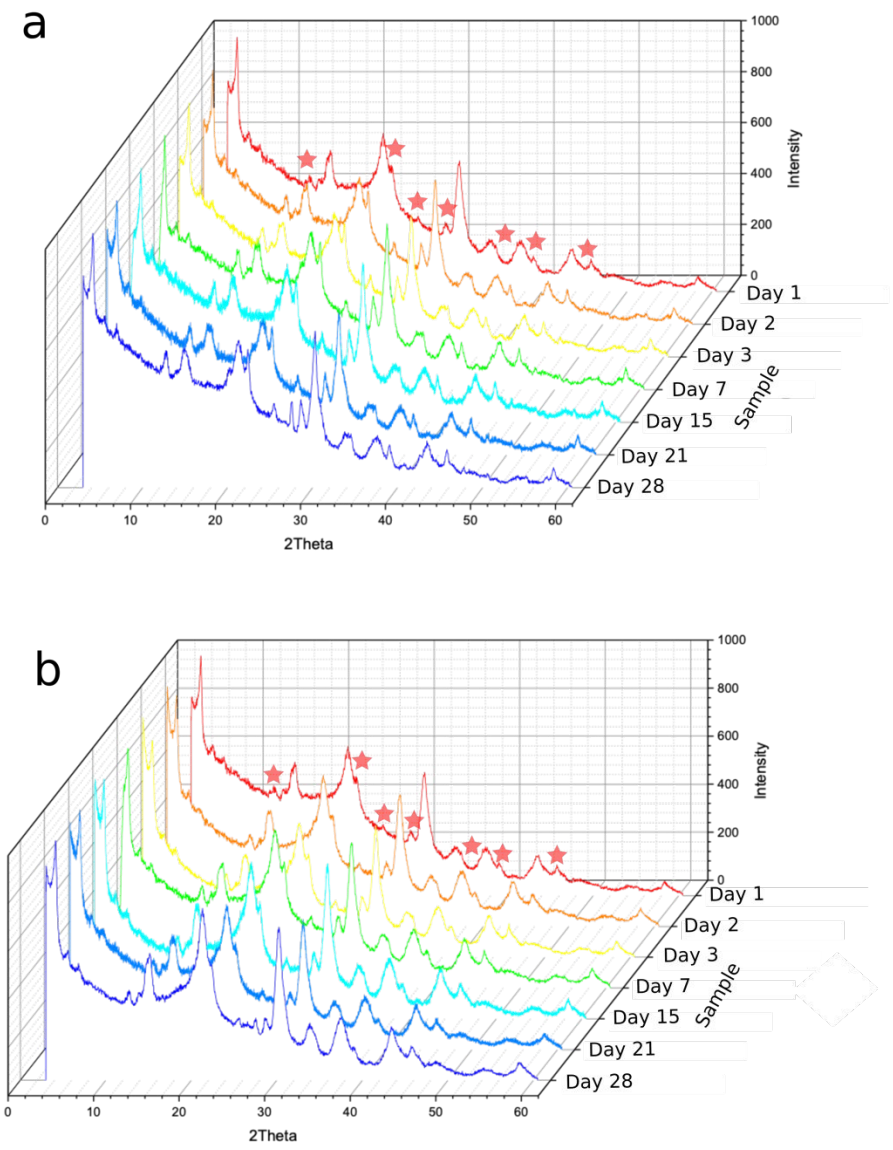

Figure S2. Monitoring the time evolution of Cs_4PbBr_6 (impurity phase) with laboratory X-ray diffraction (XRD) data of **(a)** a $CsPbBr_3$ NPLs film deposited immediately after synthesis and (**b**) $CsPbBr_3$ NPLs films deposited each time just before the measurement from the same solution. The peaks of Cs_4PbBr_6 are highlighted by red stars. As shown in (**a**), after $CsPbBr_3$ deposition the impurity amount increase from 5% w/w (day 1) up to 11% w/w (day 15) and it appears to be stable from then on. On the other hand, the solution in **(b)** shows approximately the same amount of Cs_4PbBr_6 after each deposition, suggesting that the $CsPbBr_3$ NPLs suspensions are quite stable in their colloidal state.

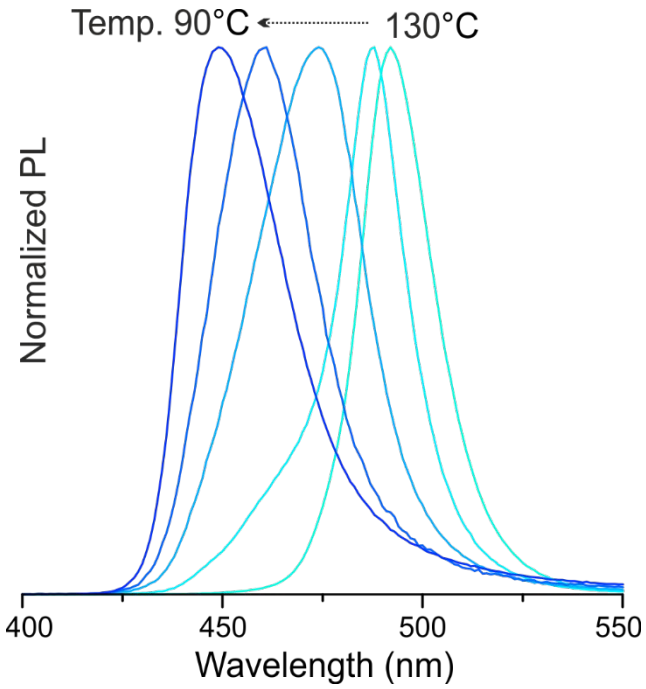

Figure S3. Normalized PL spectra of $CsPbBr_3$ NPLs with emission at 492 nm, 485 nm, 474 nm, 461 nm and 449 nm obtained by injecting Cs-oleate at 130 ºC, 120 ºC, 110 ºC, 100 ºC, and 90 ºC (from right to left).

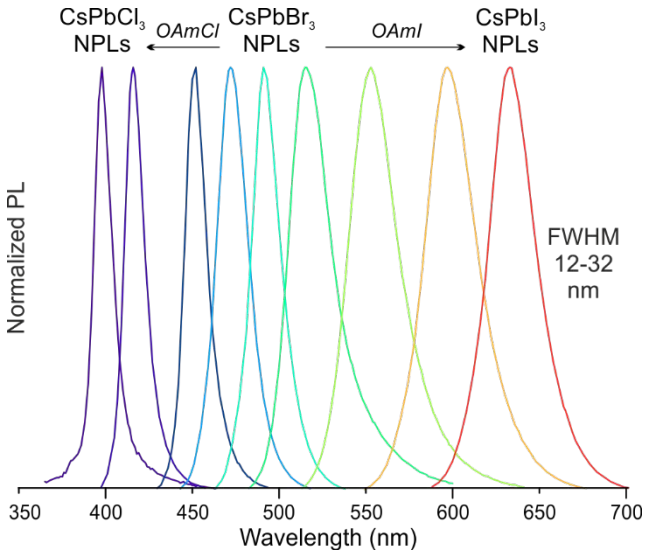

Figure S4. Normalized PL spectra for anion-exchange reactions in $CsPbBr_3$ NPLs (PL = 492 nm) using oleylammonium halides (OAmX) as halide sources. The tunability of the PL peak can be easily achieved over the entire UV-VIS spectral region by modulating the ratio between the parent NPLs and the halide source.

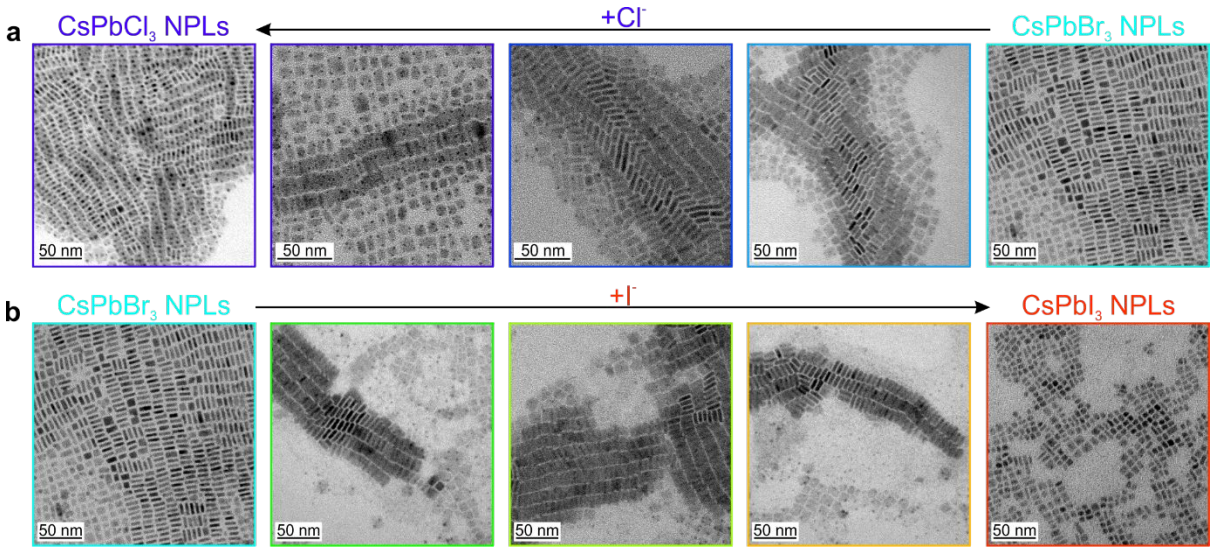

Figure S5. Transmission electron microscopy (TEM) images of $CsPbX_3$ NPLs after treatment with different amounts of (**a**) chloride and (**b**) iodide anions showing the size and shape preservation upon forming mixed-halide $CsPbBr_{3-x}Cl_x$ and $CsPbBr_{3-x}I_x$, to fully exchanged $CsPbCl_3$ and $CsPbI_3$ NPLs.

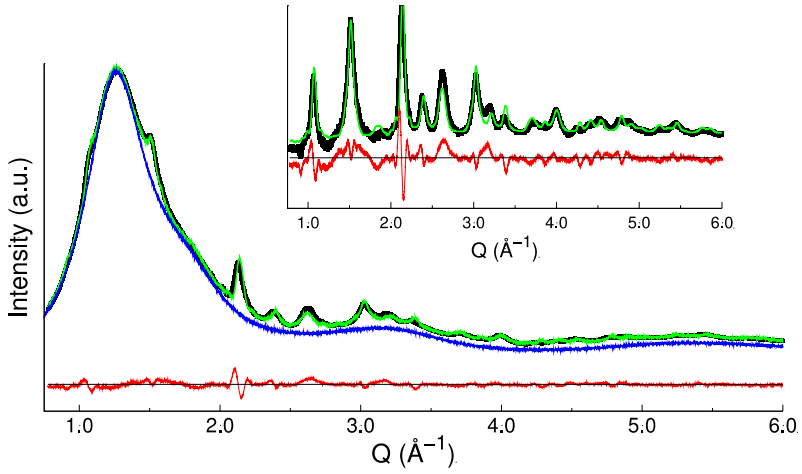

Figure S6. Synchrotron WAXTS data (black dots) of colloidal $CsPbBr_3$ NPLs in toluene (blue trace) and DSE best fit (green solid curve) obtained by using the cubic (*Pm-3m*) perovskite crystal structure (GoF=3.08). Inset: solvent-subtracted WAXTS data and DSE best fit.

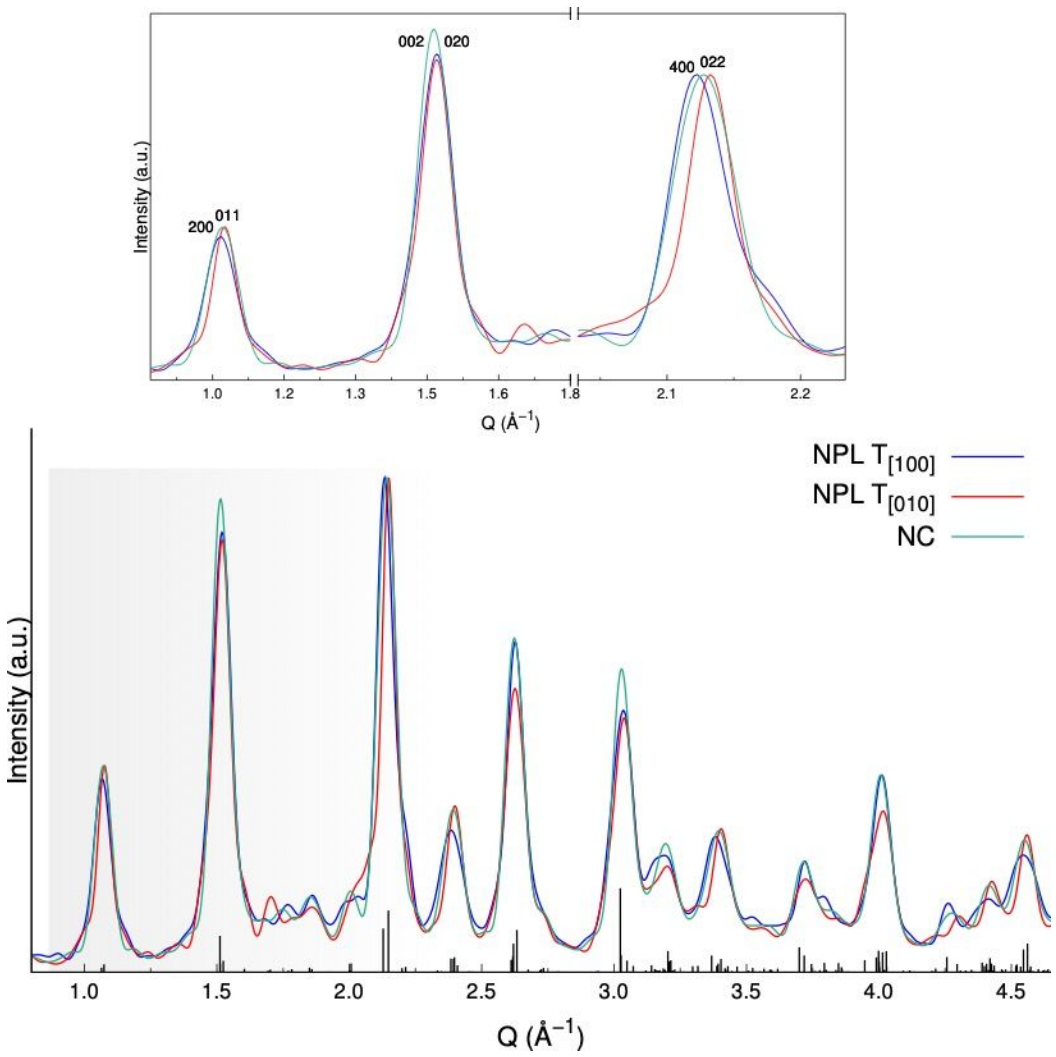

Figure S7. DSE simulations performed on $CsPbBr_3$ NPLs of 10 x10 x 3.5 nm^3 in size using the two different structure-morphology configurations ($T_{[100]}$ and $Tb_{[010]}$), as described in the main text. The DSE simulation from an isotropic nanocrystal (NC) of equivalent volume is provided for comparison. Inset: blow-up of a reduced Q-range showing how the different structure-morphology relationships cause peak shifts in the XRD patterns as a consequence of different intensity ratios among the non-equivalent reflections below each diffraction peak (very broad and not resolved, in case of NPLs or NCs). These features make it possible discriminating among the different configurations trhough DSE models and thus determine $CsPbBr_3$ NPLs structure, morphology, and their mutual relationship.

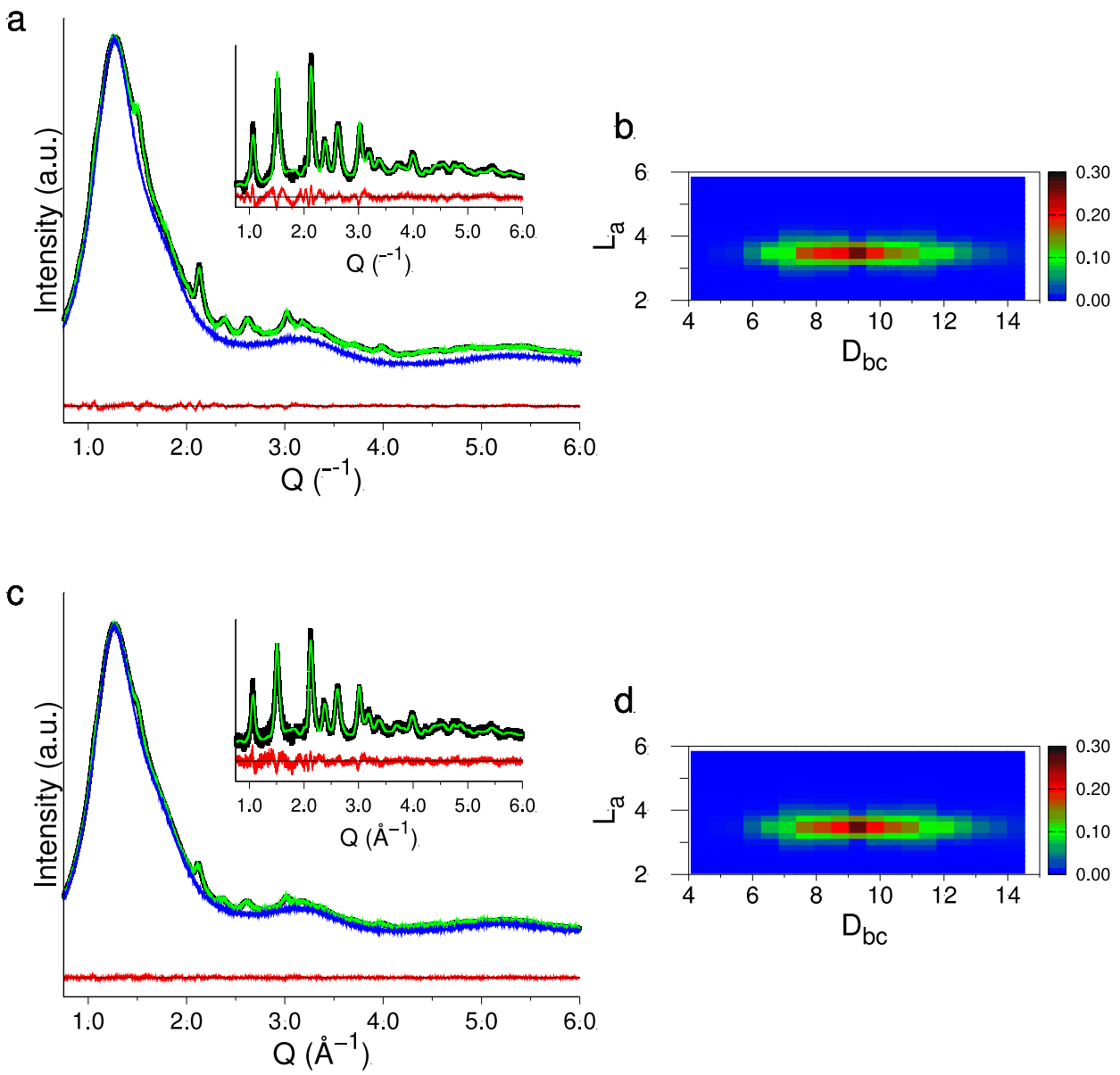

Figure S8. (a, **c)** Synchrotron WAXTS data (black dots) of colloidal $CsPbBr_3$ NPLs (different syntheses from the one reported in Figure 4 and 5 of the main text) in toluene (blue trace) and DSE best fit (green solid curve) obtained using the $T_{[100]}$ model. Insets: DSE best fit of the solvent-subtracted experimental data. **(b**, **d)** 2D maps of the bivariate log-normal size distribution functions in the L_a, D_{bc} coordinates, (L_a being the size along the thickness and D_{bc} the diameter of the circle of equivalent area to the NPLs basal plane), corresponding to the DSE bets fit shown in **(a**, **c)**. The refined number-based average size and standard deviation of the log-normal distribution functions along the two directions are: **(b)** D_{bc} = 9.83 nm (σ_{bc}/D_{bc} = 20%) and L_a = 3.50 nm (σ_a/L_a = 3.0%); **(d)** D_{bc} = 9.74 nm (σ_{bc}/D_{bc} = 22%) and L_a = 3.50 nm (σ_a/L_a = 3.0%), respectively.

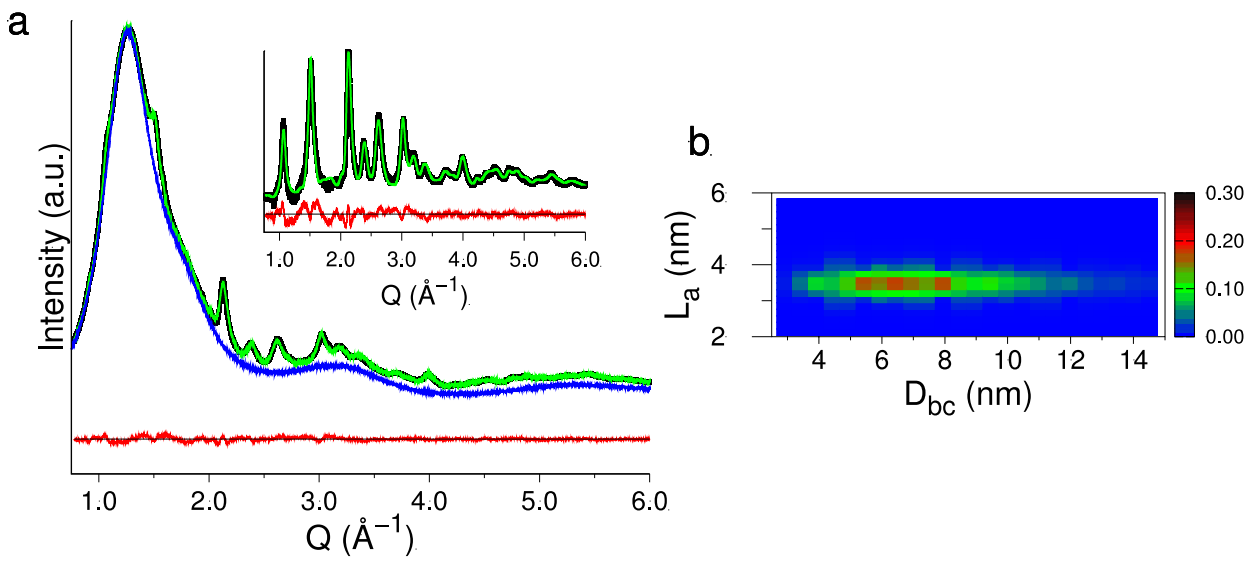

Figure S9. (**a**) DSE best fit corresponding to the minimum of the GoF isosurface (GoF=1.62) shown in Figure 4a of the main text for the $T_{[100]}$ configuration: experimental data of colloidal $CsPbBr_3$ NPLs (black dots) in toluene (blue trace), DSE simulation (green curve) and profile difference (red line). Inset: DSE best fit of the solvent-subtracted data. (**b**) 2D map of the bivariate log-normal size distribution function in the L_a, D_{bc} coordinates (L_a, D_{bc} as in Figure S8), corresponding to the DSE bets fit shown in (**a**). The refined number-based average size and standard deviation are D_{bc} = 9.0 nm (σ_{bc}/D_{bc} = 22%) and L_a = 3.5 nm (σ_a/L_a = 2.8%).

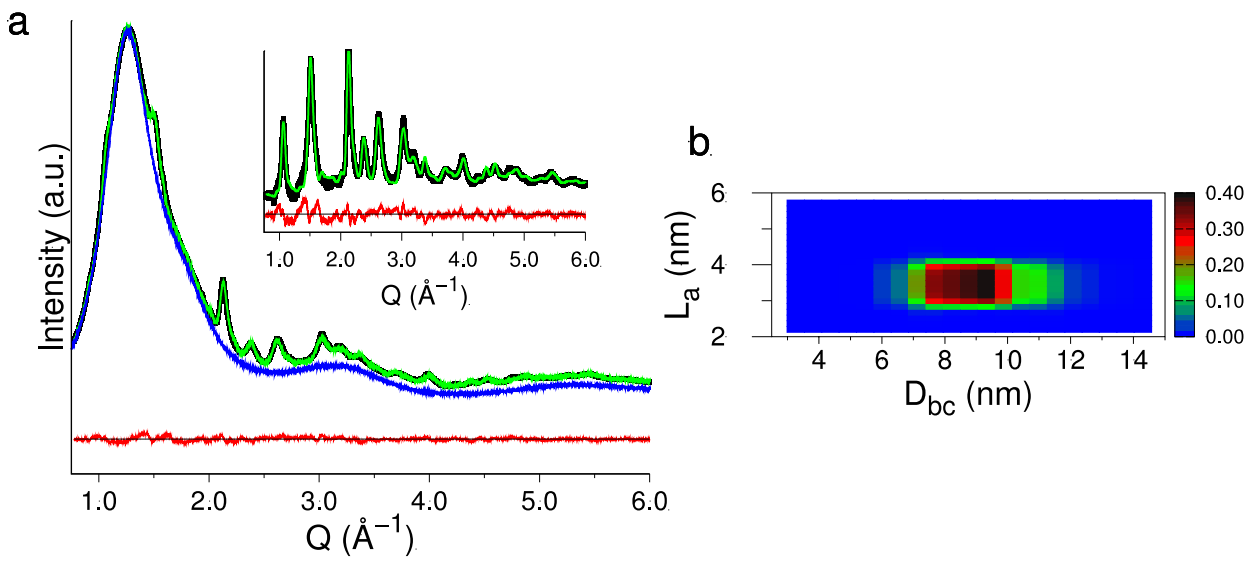

Figure S10. (**a**) DSE best fit corresponding to the minimum of the GoF isosurface (GoF=1.76) shown in Figure 4b of the main text for the $T_{[010]}$ configuration: experimental data of colloidal $CsPbBr_3$ NPLs (black dots) in toluene (blue trace), DSE simulation (green curve) and profile difference (red line). Inset: DSE best fit of the solvent-subtracted data. (**b**) 2D map of the bivariate log-normal size distribution function in the L_a, D_{bc} coordinates (L_a, D_{bc} as in Figure S8), corresponding to the DSE bets fit shown in (**a**). The refined number-based average size and standard deviation are: D_{ac} = 9.01 nm (σ_{ac}/D_{ac} =14%) and L_b = 3.50 nm (σ_b/L_b =2.0%)

Table S1. Summary of anion exchange reactions and their PL features.

$CsPbBr_3$ NPLs (5 mg/mL in toluene)	**OAmCl 1.5 mM (mL)**	**OAmI 1.5 mM (mL)**	**PL emission (nm)**	**FWHM (nm)**
0.2 mL	3.70	-	398	12.37
0.2 mL	3.10	-	406	14.02
0.2 mL	2.50	-	416	14.85
0.2 mL	1.50	-	430	15.97
0.2 mL	0.70	-	452	16.37
0.2 mL	0.30	-	472	17.71
0.2 mL	-	-	492	18.33
0.2 mL	-	0.10	515	22.13
0.2 mL	-	0.35	550	24.71
0.2 mL	-	0.60	575	27.90
0.2 mL	-	0.85	600	31.87
0.2 mL	-	1.60	632	32.78